Amphiphilic Triblock Copolymer Based on Poly(*p*-dioxanone) and Poly(ethylene glycol): Synthesis, Characterization, and Aqueous Dispersion

Remant Bahadur K. C.,[1] Santosh Aryal,[1] Shanta Raj Bhattarai,[1] Myung Seob Khil,[2] Hak Yong Kim[3]

[1]*Department of Bionanosystem Engineering, Chonbuk National University, Jeonju 561-756, Republic of Korea*
[2]*Center for Healthcare Technology Development, Chonbuk National University, Jeonju 561-756, Republic of Korea*
[3]*Department of Textile Engineering, Chonbuk National University, Jeonju 561-756, Republic of Korea*

Received 28 March 2006; accepted 27 August 2006
DOI 10.1002/app.25429
Published online in Wiley InterScience (www.interscience.wiley.com).

ABSTRACT: Amphiphilic triblock copolymers composed of poly(*p*-dioxanone) (PPDO) and poly(ethylene glycol) (PEG) were synthesized by ring opening polymerization of PDO initiated through dihydroxyl-terminated PEG in the presence of stannous 2-ethylhexanoate [$Sn(oct)_2$] as a catalyst. Polymeric nanoparticles were prepared in an aqueous medium (triple distilled water and phosphate buffer pH 7.4) by cosolvent evaporation technique at room temperature (25°C). Stability of nanoparticles was significantly enough in triple distilled water when compared with the phosphate buffer. Core-shell geometry of polymeric nanoparticles was characterized by ^{1}H-NMR spectroscopy and further confirmed by spectrophotometric analysis using pyrene as a probe. Variation in physicochemical characteristics of polymeric nanoparticles with the fraction of PPDO was investigated through the analysis of microscopic, spectroscopic, and light scattering techniques. Critical micelle concentration of polymer in triple distilled water decreased from 2.3 $\times 10^{-3}$ to 4.7 $\times 10^{-3}$. Atomic force microscopic observation revealed that polymeric nanoparticles were spherical and uniform with smooth textured of around 50–68 nm diameter. Dynamic light scattering and electrophoretic light scattering measurements showed a mono-disperse size distribution of around 113–171 nm hydrodynamic diameters and negative zeta (ζ)-potential (-4.00 to -5.87 mV), respectively. The investigation showed a significant effect of polymeric composition on the physicochemical characteristic of polymeric nanoparticles. © 2006 Wiley Periodicals, Inc. J Appl Polym Sci 103: 2695–2702, 2007

Key words: block copolymer; biomaterial; coprecipitation; nanoparticles; polymerization

INTRODUCTION

Biodegradable amphiphilic block copolymers are commonly used for the preparation of micelle type nanoparticles/drug carrier in an aqueous medium.[1,2] These polymers are self-assembled into a core-shell system (micelle) in an aqueous medium, since the medium is thermodynamically unfavorable to the hydrophobic segment.[3] In core-shell system, core serves as a reservoir for hydrophobic drugs. Mechanically, it protects the encapsulated drug from possible enzymatic degradation in the plasma during delivery. Likewise, the corona shell serves as a stabilizing interface and targeting unites. To achieve an effective response of drug, these particles should have enough circulation times in blood stream without any aggregation.[4] Large particles (>200 nm) enable their immediate reorganization as a foreign product in blood stream that causes the instant removal through the reticulo-endothelial system (RES).[5] Therefore, the particles should be small enough (<200 nm) to avoid such exclusion.[6] Similarly, surface characteristic of the particles should be ''stealthy enough'' relative to the RES cells that could limit the possible opsonization.[7]

Indeed, many reports regarding the formulation of polymeric nanoparticles of controlled size using biodegradable amphiphilic block copolymers have been published. Among them, aliphatic polyesters with poly(ethylene glycol) (PEG) as a hydrophilic segment, viz, PLA-*b*-PEG,[8] PCL-*b*-PEG,[9] and PLGA-*b*-PEG[10] have been synthesized and frequently applied as a polymeric nanocarrier in drug delivery system. An important realization in the formation of polymeric nanoparticles is to cover them with nonionic hydrophilic polymers such as poly(*N*-vinylpyrrolidone), PEG, dextrane, chitosan, etc.[11–14] Among them, PEG has a significant attention because of its well-known physicochemical and biological proper-

Correspondence to: H. Y. Kim (khy@moak.chonbuk.ac.kr).
Contract grant sponsors: Korean Research Foundation (KRF), Korean Government (MOEHRD), Korean Ministry of Educational and Human Resources Development.

TABLE I
Characterization of PPDO-*b*-PEO-*b*-PPDO Block Copolymer

Samples	M_n of PEG	Polydispersity of PEG (M_w/M_n)[a]	Feed ratio (wt %)		Composition (wt %)[b]		M_n[a]	M_w[a]	Polydispersity (M_w/M_n)[a]
			PEG	PDO	PEG	PPDO			
R_1	2000	1.24	5	95	7.50	92.50	8870	19,900	2.24
R_2	3500	1.21	10	90	13.65	86.35	13,700	25,200	1.83
R_3	6000	1.13	15	85	20.64	79.36	21,360	41,011	1.92
R_4	10,000	1.20	20	80	24.10	75.90	39,784	49,730	1.25

[a] Measured by GPC analysis.
[b] Determined from ^{1}H-NMR spectroscopy ($CDCl_3$).

ties.[15,16] PEG has also received the attention of Food and Drug Administration (FDA) for its possible internal consumption.[17] PEG shell, covalently linked with hydrophobic core can increase the stability of polymeric nanoparticles in biological environment and minimize the possible mechanical clearance in RES. So far, research works have been focused mainly on the preparation of polymeric nanoparticles using aliphatic polyesters. Less attention has been paid for the preparation of poly(ester-*alt*-ether)-based polymeric nanoparticles for which poly(1,4-dioxan-2-one) (PPDO) could be an excellent polymer.

PPDO is a well-known biodegradable and biocompatible poly(ester-*alt*-ether) polymer with superior mechanical properties and finds application as a complementary to other biodegradable aliphatic polyesters.[18] Block copolymers consisting PPDO moieties attached at two ends of PEG has been well-described.[19] Synthesis and *in vitro* degradation of copolymers of PDO with glycolide and thermal properties of copolymers of PDO with PEG have been well reported in our previous publication[20,21] However, the higher conversion of PDO into copolymer is still a challenging task because of its low reactivity at higher temperature.[22] It has been reported that PDO undergoes polymerization through equilibrium, i.e., PDO and PPDO are easily polymerizable and depolymerizable materials, respectively.[23,24] Therefore, the effective conversion of PDO into copolymer is still a challenging task.[22] The objective of this research was to synthesize an amphiphilic triblock copolymer, poly(*p*-dioxanone)-*b*-poly(ethylene oxide)-*b*-poly(*p*-dioxanone) (PPDO-*b*-PEG-*b*-PPDO) and to prepare nanoparticles in aqueous medium. Polymerization and molecular composition of polymer were characterized by different physicochemical techniques (GPC, ^{1}H-NMR, FTIR, TGA, and DSC). Polymeric nanoparticles were characterized with ^{1}H-NMR, fluorescence spectrophotometric analysis, atomic force microscopic (AFM), dynamic light scattering (DLS), and electrophoretic light scattering (ELS) methods.

EXPERIMENTAL

Materials

PEG (M_n = 2000, 3500, 6000, and 10,000) (Aldrich Chemical Co.) was used after re-precipitation using dichloromethane and diethyl ether as solvent and non-solvent, respectively, and azeotropic distillation was performed to remove the moisture. PDO provided by Meta Biomedical Co., Korea, was used as received. $Sn(oct)_2$ (Aldrich Chemical Co.) was used after being dissolved in dry toluene (0.039*M*). All the other chemicals used in this research were purchased from Showa Chemical, Japan.

Polymer synthesis

PPDO-*b*-PEO-*b*-PPDO triblock copolymers of different composition (Table I) were synthesized by ring opening polymerization of PDO in the presence of $Sn(oct)_2$ as a catalyst as described earlier.[21] Briefly, in typical experiment, $Sn(oct)_2$ (0.45 mL) was introduced into three-necked round-bottom flask containing predried PEG and heated for 1 h at 100°C to ensure complete drying and then cooled down to room temperature (25°C) using argon. PDO was then injected to the flask. The flask was evacuated for 3 h and degassed with argon for 1 h. Reaction mixture was stirred for 1 h at 90°C and left at 80°C for 30 h, and the mass thus obtained was dissolved in hexafluoroisopropanol (HFIP), precipitated in cold methanol, and repeatedly washed with cold diethyl ether.

Preparation of PPDO-*b*-PEO-*b*-PPDO nanoparticles

PPDO-*b*-PEO-*b*-PPDO nanoparticles were prepared by cosolvent evaporation technique.[25] HFIP was selected as a solvent for R_1, R_2, and R_3, whereas both acetonitrile and HFIP were selected for R_4 for the preparation of nanoparticles. The polymer (5.0 mg) was dissolved in organic solvent (1.0 mL) and dropped into aqueous medium (5.0 mL) (triple dis-

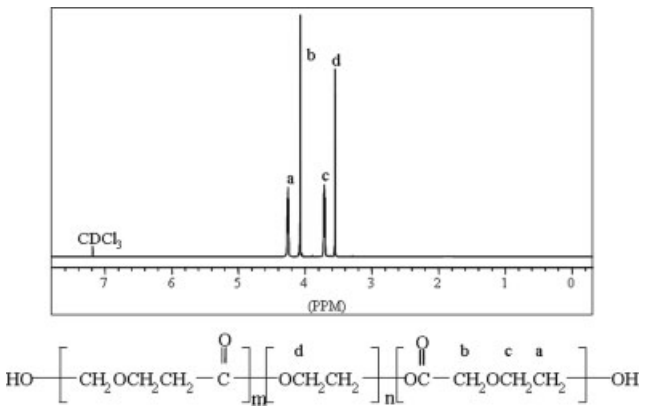

Figure 1 ^{1}H-NMR spectra of PPDO-*b*-PEO-*b*-PPDO (R_4), 6% (w/v) solution in $CDCl_3$ using TMS as the internal reference.

tilled water or phosphate buffer at pH 7.4) under moderate stirring (50 rpm) at room temperature (25°C). Organic phase was allowed to evaporate under reduced pressure until final volume of nanoparticles suspension was reduced to 5 mL. Finally, the nanoparticles suspension was filtered through microfilter with 0.2 μm pore size.

Characterization

Polymer characterization

Gel permeation chromatography (GPC) measurement was done on Waters 150C equipped with a refractive index detector and Waters Styragel® columns (HR_1, HR_2, and HR_4) with size 7.8 × 300 nm using chloroform as a mobile phase at a flow rate of 1.0 mL/min. Nuclear magnetic resonance (^{1}H-NMR) spectrum was recorded in JNM-Ex 400 FT-NMR spectrometer operating at 400 MHz; 6% (w/v) solution in $CDCl_3$ using tetramethyl silane (TMS) as a internal reference. Fourier-transform infrared (FTIR) spectra were recorded as KBr pellets using an ABB Bomen MB 100 spectrometer. Thermogravimetric analysis (TGA) was done by a TA 2010 type thermogravimetric analyzer at the heating rate of 15°C/min in the range of 50–600°C under the steady flow of nitrogen. Differential scanning calorimetric (DSC) analysis of polymer was done by a DSC Q100 V7.3 Build 249 (DSC standard cell) at a heating rate of 20°C/min in the range of −90 to 150°C under the steady flow of nitrogen.

Nanoparticles characterization

^{1}H-NMR spectrum was recorded in JNM-Ex 400 FT-NMR spectrometer operating at 400 MHz at room temperature in deuterium oxide (D_2O) using TMS as an internal reference. The steady-state fluorescent excitation spectra (λ_{em} = 390 nm) of pyrene were measured at various polymer concentrations using a F-200 Fluorescence Spectrophotometer 2510221-07 (Hitachi, Japan) for the measurement of critical micelle concentration (CMC). Concentrations of polymer and pyrene were in the range of 1×10^{-4} to 1 g/L and $6 \times 10^{-7}M$ in triple distilled water (pH 7.4), respectively. Size and surface characteristics of polymeric nanoparticles were observed in AFM Nanoscope IV multimode (Digital instrument, Mikro masch, USA) in tapping mode using a Si cantilever with a spring constant of 3.5 N/m and a resonance frequency of 75 kHz. Scanning was performed at a scan speed of 1.85 Hz with a resolution of 512 × 512 pixels. Samples for AFM observation were prepared as a drop-coated film on the argon dried Si (111) wafers. DLS (Malvern System 4700) measurement was performed to analyze the average particle size and size distribution at measuring angle 90° to the vertically polarized argon-ion laser (Cyonics). ζ-potential of particles was determined in electrophoretic light scattering spectrophotometer (ELS 8000/6000 Otsuka electronics Co.) measuring angle at 20° to the incident beam. Each measurement was performed after the appropriate dilution (four times of initial volume) of nanoparticles particle suspension in triple distilled water at room temperature. Particle dispersion was sonicated in a bath of an ultrasonicator for 1 min before each analysis.

RESULTS AND DISCUSSION

Molecular weight distribution and composition of the polymers were determined using GPC and ^{1}H-NMR spectroscopy, respectively. Feed ratio (PEG/PDO) and the results of polymerization are summarized in Table I. All the polymers showed relatively wide

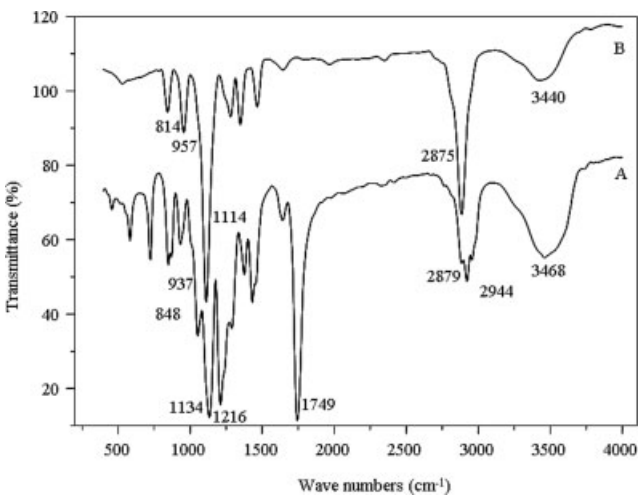

Figure 2 FTIR spectra recorded from KBr plate of, PPDO-*b*-PEO-*b*-PPDO (R_4) (A) and PEG (10,000) (B).

TABLE II
Thermal Properties of PPDO-*b*-PEO-*b*-PPDO Block Copolymer Derived from DSC Analysis

Samples	1st run (°C)			2nd run (°C)		
	T_m	T_c	T_g	T_m	T_c	T_g
R_1	109.93	–	–	107.5	32.97	–
R_2	104.50	–	–	101.90	29.41	−23.19
R_3	105.20	–	–	103.87	24.38	−21.92
R_4	107.67	–	–	100.84	22.80	−23.33

T_m, T_c, and T_g, are the melting, crystallization, and glass transition temperature of the polymers.

molecular weight distribution and polydispersity [M_w/M_n] from 1.25 to 2.24 (spectra not shown). This fact might be caused by the possible intermolecular ester interchange at high temperature, till the establishment of the most probable molecular mass distribution.[26] Polydispersity was found to increase with the PPDO fraction in the polymer.

Typical ^{1}H-NMR spectra (Fig. 1) of PPDO-*b*-PEO-*b*-PPDO exhibit two sharp and distinct singlet centered at δ 4.06 and 3.55 ppm and two equally intense triplets at δ 4.25 and 3.71 ppm. Singlet resonance at δ 3.55 ppm corresponds to the —O—CH_2CH_2—O— unit of PEO segment. Singlet resonances at δ 4.06 ppm and triplet resonance at δ 4.25 and 3.71 ppm correspond to —O—CH_2—CO—, —O—$CH_2$$CH_2$—OCO— and —O—$CH_2$$CH_2$—OCO— units of PPDO segment, respectively. Intensity of resonance at δ 3.55 ppm was linearly increased with the content of PEG, which implies the substantial increase in hydrophilic segment (PEO) in polymer. Further, the absence of resonance signals at δ 5.0–4.9 and 4.03 ppm indicates the absence of any type of carboxylic acid fractions in polymers. Mole fraction of repeating units and molecular weight of all the polymers were determined from the well-resolved resonance at δ 4.06 and 3.55 ppm protons of PPDO and PEO segments, respectively. These spectral features corresponding to the PPDO and PEG units indicate their presence in the copolymer.

FTIR spectra of polymer (R_4) along with PEG (M_n = 10,000) are as shown in Figure 2. Copolymer exhibited the characteristic intense bands at 1134, 1216, and 1749 cm^{-1}, and broad bands at 2879–2944 and 3468 cm^{-1}. C—H stretching vibration (2875 cm^{-1}) and C—O—C bending vibration (1114 cm^{-1}) of PEG has been shifted to 2879 and 1134 cm^{-1}, respectively, as it was polymerized with PDO.[27] Stretching vibration at 1749 and 2944 cm^{-1}, attributed to the carbonyl group (C=O stretching vibration of homopolymer PPDO at 1733 cm^{-1}) and aliphatic C—H chain, respectively, corresponding to the PPDO segment were well resolved in copolymer spectra (Curve B).[22] Similarly, the bands at 3468 and 1032 to 1304 cm^{-1}attributed to the terminal —OH, and C—O—C and C—O—CO group, respectively, were well resolved in the spectra of copolymer (Curve B). Intensity of C—H stretching at 2879 cm^{-1} (PEO) was linearly increased with the content of PEG when compared with the aliphatic C—H stretching at 2944 cm^{-1} (PPDO). The bands at 814 and 957 cm^{-1} known as the characteristic crystalline phase of PEG has shifted significantly to 848 and 937 cm^{-1}, respectively, suggesting that the crystallinity of PEO segment was influenced by the PPDO

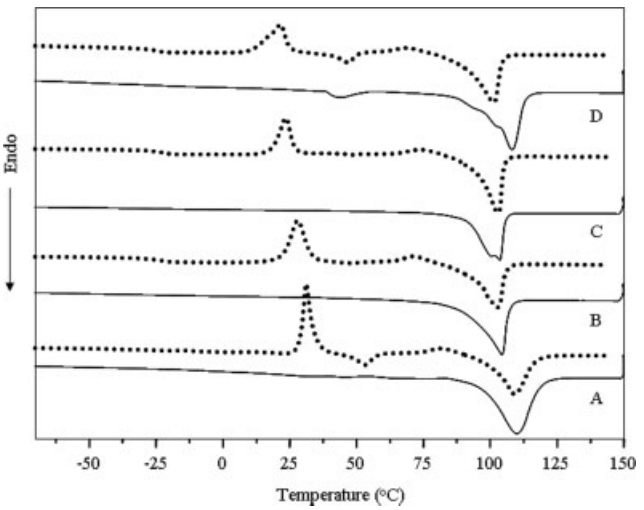

Figure 3 DSC thermograms of PPDO-*b*-PEO-*b*-PPDO (R_1) (A), PPDO-*b*-PEO-*b*-PPDO (R_2) (B), PPDO-*b*-PEO-*b*-PPDO (R_3) (C), and PPDO-*b*-PEO-*b*-PPDO (R_4) (D) obtained by heating the samples from −90 to 150°C at 20°C/min under the steady flow of nitrogen. Solid line (—) represents the 1st run DSC thermograms of the polymers and dot lines (·····) represent the 2nd run thermograms after quenching the polymers in liquid nitrogen.

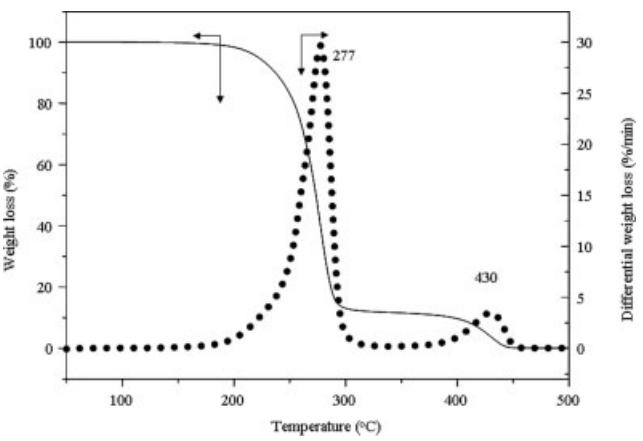

Figure 4 TG curve of PPDO-*b*-PEO-*b*-PPDO (R_4) obtained by heating the samples from 50 to 600°C at 15°C/min under the steady flow of nitrogen. Solid line (—) represents the TGA curve and dot lines (••••) represent the DTA curve.

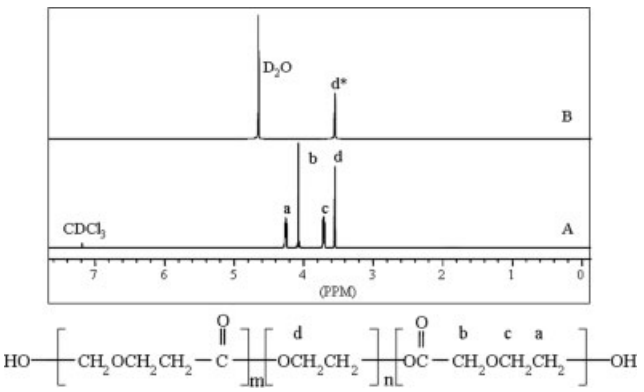

Figure 5 ^{1}H-NMR spectrum of PPDO-*b*-PEO-*b*-PPDO (R_4), 6% (w/v) solution in $CDCl_3$ (A) PPDO-*b*-PEO-*b*-PPDO (R_4) nanoparticles dispersed in D_2O (1 mg/mL) (B) using tetramethyl silane as the internal reference.

fraction.[22] These spectral features corresponding to the PPDO and PEG units indicate their presence in the copolymer.

Thermal characteristics of copolymer analyzed through DSC are summarized in Table II. Glass transition temperature (T_g) and crystallization temperature (T_c) of the copolymer were resolved only in 2nd run, whereas the melting temperature (T_m) was resolved in both 1st and 2nd run DSC thermograms (Fig. 3). Results showed that T_c of polymer linearly decreased with the molecular weight of PEG, whereas the T_g and T_m remained nearly constant. The single T_g, T_c, and T_m obtained for different copolymer imply the complete miscibility of all the segments within the copolymers.

Thermogravimetric analysis is the best method for the characterization of copolymers.[28] Composition of the repeating units in copolymer can be obtained by the thermal degradation process illustrated through inflection point temperature (T_d) and percentage weight loss (ΔW). TG curve of the copolymer (R_4) presented in Figure 4, showed two distinct weight loss steps. The calculated values of T_d and ΔW suggest that the first degradation step was due to PPDO segment and the second one was due to PEO segment. T_d of the PPDO was observed at 277°C, whereas that of PEO at 430°C. It implies the presence of two distinct blocks in polymer, thereby supporting the effectiveness of block polymerization.

Self-assembly of amphiphilic block copolymers can be accomplished by different techniques, viz, direct dissolution, solvent evaporation/film formation, dialysis, cosolvent evaporation, etc.[1,25] In the present study, we have selected cosolvent evaporation technique (acetonitrile/water and HFIP/water system depending on the solubility of polymer). Samples R_1, R_2, and R_3 were soluble only in HFIP, whereas samples R_4 was soluble in both acetonitrile and HFIP. Particles of R_1, R_2, and R_3 prepared in phosphate buffer were stable up to 1 week, and the particles of R_4 were stable up to 1 month (data not shown). On the other hand, the particles of R_1 and R_2 were stable up to 2 weeks, and the particles of R_3 were stable up to almost 1 month, as it was prepared in triple distilled water. Similarly, the stability of particles of R_4 was more than 1 month, while it was prepared in triple distilled water (data not shown). It indicates the effect of ions and the content of hydrophilic segment on the stability of polymeric nanoparticles.[29] Furthermore, we did not find any significant variation in the particles size and morphology of the sample R_4 prepared using acetonitrile/water and HFIP/water system, which indicated the independence of solvent. The increased stability of nanoparticles with

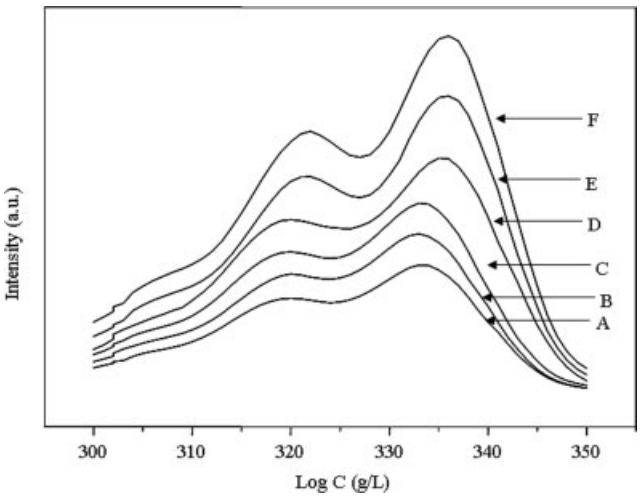

Figure 6 Fluorescence excitation spectra of pyrene in triple distilled water (pH 7.4) as a function of PPDO-*b*-PEO-*b*-PPDO (R_4) nanoparticles concentration; 0.0001 (A), 0.0015 (B), 0.01 (C), 0.065 (D), 0.4 (E), 1.0 (F) mg/mL (λ_{em} 390.0 nm).

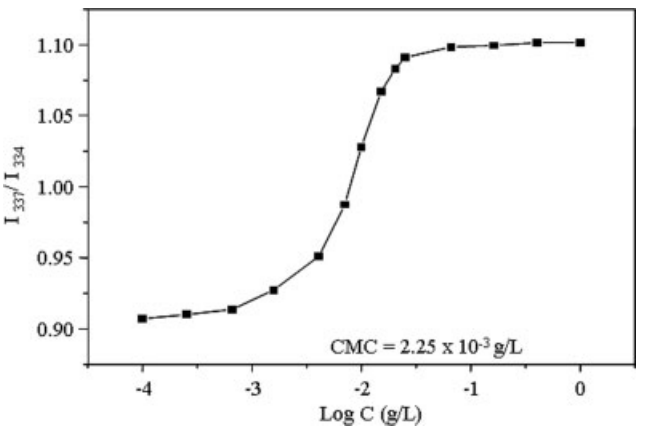

Figure 7 Intensity ratio (I_{337}/I_{334}) from pyrene (6×10^{-7} m) excitation spectra (λ_{em} 390.0 nm) versus nanoparticles concentration (log *C*) in triple distilled water (pH 7.4): PPDO-*b*-PEO-*b*-PPDO (R_4).

TABLE III
Characterization of PPDO-*b*-PEO-*b*-PPDO Nanoparticles

Samples	Particle size (nm)		ζ-Potential (mV)	Polydispersity	CMC (g/L)
	AFM	DLS			
R_1	68 ± 0.6	171 ± 2.6	−5.87 ± 0.15	0.20 ± 0.05	$4.7 \times 10^{-3} \pm 0.02$
R_2	56 ± 0.4	130 ± 2.9	−4.85 ± 0.09	0.13 ± 0.07	$5.3 \times 10^{-3} \pm 0.03$
R_3	54 ± 0.2	120 ± 2.5	−4.74 ± 0.12	0.13 ± 0.03	$3.5 \times 10^{-3} \pm 0.01$
R_4	50 ± 0.5	113 ± 2.3	−4.00 ± 0.14	0.13 ± 0.02	$2.2 \times 10^{-3} \pm 0.02$

$n = 3$. All values are expressed as mean ± SD.

the molecular weight of PEG was due to its stabilizing effect,[1] whereas the decreased stability with the content of PPDO could be due to increase in cyrstallinity. Water permeability of a system increases with the crystallinity that consequently leads the hydrolysis of the polymers.

Resonance peaks at δ 4.25, 4.06, and 3.71 ppm corresponding to PPDO in $CDCl_3$ were completely disappeared except the singlet at δ 3.55 in D_2O corresponding to PEO (Fig. 5). All the characteristic resonances in $CDCl_3$ (Spectrum A) were in good agreement with the basic structure of polymer, whereas

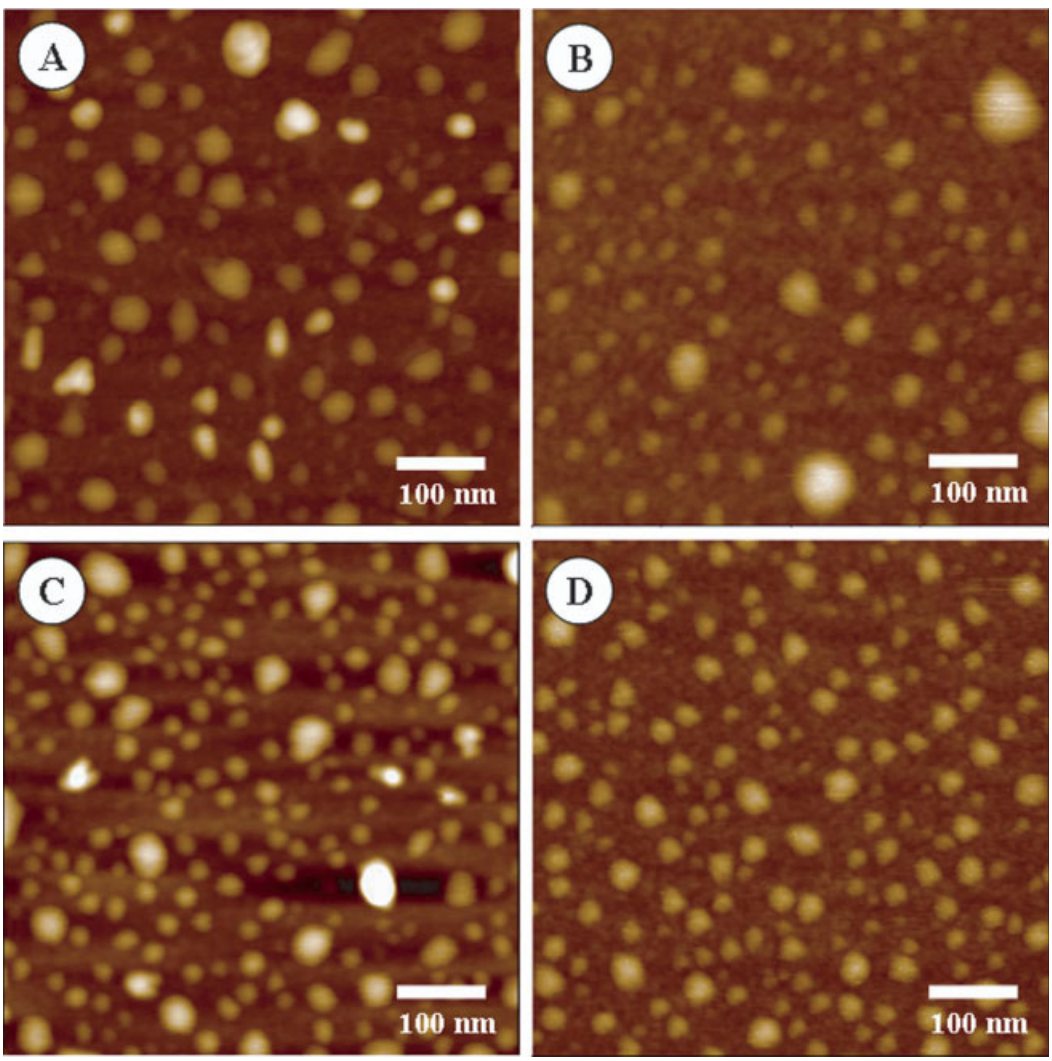

Figure 8 AFM image recorded from the drop-cast film of PPDO-*b*-PEO-*b*-PPDO (R_1) (A), PPDO-*b*-PEO-*b*-PPDO (R_2) (B) PPDO-*b*-PEO-*b*-PPDO (R_3) (C) and PPDO-*b*-PEO-*b*-PPDO (R_4) (D) polymeric nanoparticles dispersed in triple distilled water (pH 7.4) (1 mg/mL). [Color figure can be viewed in the online issue, which is available at www.interscience.wiley.com.]

the existence of only one signal (*d**) at δ 3.55 ppm in D_2O (Spectrum B) was allied to the basic structure of nanoparticles. Such variation may be only due to the complete masking of hydrophobic segment in aqueous medium, which implies the modification of polymer into self-assembled core-shell system. Furthermore, the existence of hydrophobic domain as a core of nanoparticles was investigated by the spectrophotometric analysis using pyrene as a prob.

Steady-state pyrene fluorescence method was used for the determination of CMC of polymer.[30] Fluorescence excitation spectra of pyrene (triple distilled water pH 7.4) in various polymeric concentrations (sample R_4) are presented in Figure 6. The linear red shift found in the spectra with the concentration of polymer was because pyrene was preferentially partitioned into hydrophobic domains and moved from polar environment to hydrophobic micelle cores.[31] CMC of polymer was determined by plotting the intensity ratios (I_{337}/I_{334}; 0,2 and 0,0 bands, respectively) versus polymer concentration (log *C*). At low polymer concentrations, these ratios give the value of pyrene in hydrophilic environment and at high concentration it gives the value of pyrene in the hydrophobic environment (Fig. 7). The CMC value of the polymer was slightly decreased with the fraction of PPDO (Table III). It indicates the formation of micelle was facilitated by fraction of hydrophobicity of polymer.[32]

For the application of polymeric nanoparticles in various biomedical fields for sustainable drug release, particle size, stability, and surface characteristics are the important factors.[2,21,25] Figures 8(A)–8(D) show the AFM images of different polymeric nanoparticles. AFM observation of particles reveals that most of the particles from all the samples were discrete, smooth, and regular with 50–68 nm diameter. However, the particles of R_1 and R_2 were not so regular when compared with R_3 and R_4. Morphology and size distribution of R_3 and R_4 were nearly identical as it can be seen in Figures 8(C) and 8(D). It implies that the morphology and distribution of particle is dependent on the content and size of hydrophilic segment (Table III).[1]

Size distribution of polymeric nanoparticles measured by DLS is presented in Figures 9(A)–9(D). DLS measurement shows a unimodal size distribution with mean hydrodynamic diameter in the range of 113–171 nm (Table III). Particle size was significantly decreased with molecular weight of PEG, which was in a good agreement with the AFM observation. The wide variation in the size dimension measured by AFM and DLS may be due to the fact that DLS measurement gives only hydrodynamic diameter rather than the actual diameter. ζ-potential is one of the most important physicochemical characteristics of polymeric nanoparticles. In the present study, ζ-potential showed a negative correlation with PPDO content due to the increase in ionizable carboxyl groups (Table III).[33] Despite of small surface charge, stability of polymeric nanoparticles was linearly increased with the molecular weight of the PEG because of the solubilization effect of PEG.

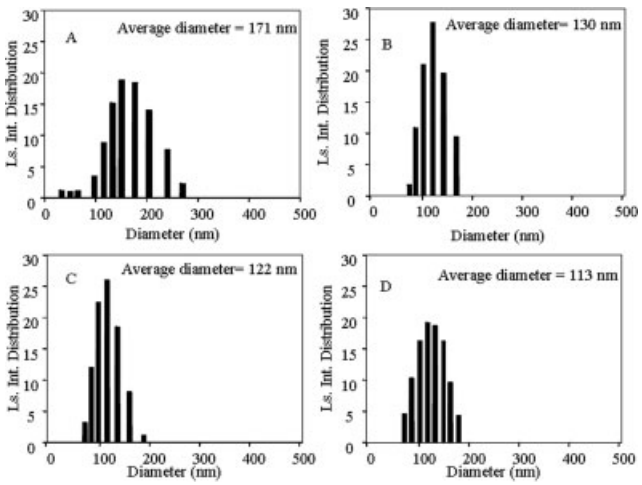

Figure 9 Size distribution measured from PPDO-*b*-PEO-*b*-PPDO (R_1) (A), PPDO-*b*-PEO-*b*-PPDO (R_2) (B) PPDO-*b*-PEO-*b*-PPDO (R_3) (C) and PPDO-*b*-PEO-*b*-PPDO (R_4) (D) nanoparticles dispersed in triple distilled water (pH 7.4) (1 mg/mL).

CONCLUSIONS

ABA types biodegradable amphiphilic triblock copolymers, poly(*p*-dioxanone)-*block*-poly(ethylene oxide)-*block*-poly(*p*-dioxanone) (PPDO-*b*-PEO-*b*-PPDO) were synthesized by ring opening polymerization of *p*-dioxanone through the dihydroxyl-terminated PEG in the presence of $Sn(oct)_2$ as a catalyst. Well-dispersed polymeric nanoparticles were prepared in aqueous medium (triple distilled water and phosphate buffer) pH 7.4 at room temperature by cosolvent evaporation technique. AFM observation and light scattering measurement (DLS and ELS) revealed that the physicochemical properties of the polymeric nanoparticles were affected by the molecular composition of the copolymers. The ionic feature of formulation medium exclusively influenced the stability of polymeric nanoparticles. Hence, we believe that these poly(ester-*alt*-ether) block-based polymeric nanoparticles of desired dimension could be formulated in required medium.

References

1. Allen, C.; Maysinger, D.; Eisenberg, A. Colloids Surf B 1999, 16, 3.
2. Brigger, I.; Dubernet, C.; Couvreur, P. Adv Drug Delivery Rev 2002, 54, 631.

3. Tuzar, Z.; Kratochvil, P. Adv Colloid Interface Sci 1976, 6, 201.
4. Kossovski, N.; Millet, D.; Gelman, A.; Sponsler, E.; Hnatyszyn, H. J Biotechnol 1993, 11, 1534.
5. Grislain, L.; Couvreur, P.; Lenaerts, V.; Roland, M.; Deprez-Decampeneere, D.; Speiser, P. Int J Pharm 1983, 15, 335.
6. Petrak, K. Drugs Pharm Sci 1993, 61, 275.
7. Kim, S. Y.; Shin, I. L. G.; Lee, Y. M.; Cho, C. S.; Sung, Y. K. J Controlled Release 1998, 51, 13.
8. Govender, T.; Riley, T.; Ehtezazi, T.; Garnett, M. C.; Stolink, S.; Illum, L.; Davis, S. S. Int J Pharm 2000, 199, 95.
9. Ge, H.; Hu, Y.; Jiang, X.; Cheng, D.; Yuan, Y.; Bi, H.; Yang, C. J Pharm Sci 2002, 91, 1463.
10. Gref, R.; Minamitake, Y.; Peracchia, M. T.; Trubetskoy, V.; Torchilin, V.; Langer, R. Science 1994, 263, 1600.
11. Luo, L.; Ranger, M.; Lessard, D. G.; Garrec, D. L.; Gori, S.; Leroux, J. C.; Rimmer, S.; Smith, D. Macromolecules 2004, 37, 4008.
12. Kabanov, A. V.; Batrakova, E. V.; Alakhov, V. Y. Adv Drug Delivery Rev 2002, 54, 759.
13. Osterberg, E.; Bergstrom, K.; Holmberg, K.; Schuman, T. P.; Riggs, J. A.; Burns, N. L.; Alstine, J. M. V.; Harris, J. M. J Biomed Mater Res 1995, 29, 741.
14. Ruel-Gariepy, E.; Leclair, G.; Hildgen, P.; Gupta, A.; Leroux, J. C. J Controlled Release 2002, 82, 373.
15. Herold, D. A.; Keli, K.; Bruns, D. E. Biochem Pharmacol 1989, 38, 73.
16. Richter, A. W.; Akerblom, E. Arch Allergy Appl Immunol 1987, 38, 73.
17. Schact, E. H.; Hoste K. In Poly(ethylene glycol); Harris, J. M.; Zaplipsky, S., Eds.; ACS Symposium Series; American Chemical Society: Washington, DC, 1997; p 297.
18. Huatan, H.; Collett, J. H.; Attwood, D. J Micorencapsulation 1995, 12, 557.
19. Wang, H.; Dong, J. H.; Qiu, K. Y.; Gu, Z. W. J Appl Polym Sci 1998, 68, 2121.
20. Bhattarai, N.; Jiang, W. Y.; Kim, H. Y.; Lee, D. R.; Park, S. J. J Polym Sci Part B: Polym Phys 2004, 42, 2558.
21. Bhattarai, N.; Kim, H. Y.; Cha, D. I.; Lee, D. R.; Yoo, D. I. Eur Polym J 2003, 39, 1365.
22. Bhattarai, N.; Kim, H. Y.; Lee, D. R.; Park, S. J. Polym Int 2003, 52, 6.
23. Nishida, H.; Yamashita, M.; Endo, T.; Tokiwa, Y. Macromolecules 2000, 33, 6982.
24. Kricheldorf, H. R.; Damrau, D. O. Macromol Chem Phys 1998, 199, 1089.
25. Bhattarai, N.; Bhattarai, S. R.; Khil, M. S.; Lee, D. R.; Kim, H. Y. Eur Polym J 2003, 39, 1603.
26. Cerrai, P.; Tricoli, M.; Andruzzi, F.; Poci, M.; Pasi, M. Polymer 1989, 30, 338.
27. Rashkov, I.; Manolova, N.; Li, S. M.; Espartero, J. L.; Vert, M. Macromolecules 1996, 29, 50.
28. Bhattarai, N.; Kim, H. Y.; Lee, D. R. Polym Degrad Stab 2002, 78, 423.
29. Jain, N. J.; Aswal, V. K.; Goyal, P. S.; Bahadur, P. Colloids Surf A 2000, 173, 85.
30. Wilhelm, M.; Zhao, C. L.; Wang, Y.; Xu, R.; Winnik, M. A.; Mura, J. L.; Riess, G.; Croucher, M. D. Macromolecules 1991, 24, 1033.
31. Zhao, C. L.; Wang, Y.; Winnik, M. A.; Riess, G.; Croucher, M. D. Langmuir 1990, 6, 514.
32. Gao, Z.; Eisenberg, A. Macromolecules 1993, 26, 7353.
33. Riley, T.; Govender, T.; Stolnik, S.; Xiong, C. D.; Garnett, M. C.; Illum, L.; Davis, S. S. Colloids Surf B 1999, 16, 147.